

Rb₂Hg₃Te₄: A New Layered Compound Synthesized from Solvothermal Reactions

Jing Li,^{*,†} Zhen Chen, and Kin-Chung Lam

Department of Chemistry, Rutgers University, Camden, New Jersey 08102

Suzanne Mulley and Davide M. Proserpio*

Dipartimento di Chimica Strutturale e Stereochimica Inorganica, Università di Milano, 20133 Milano, Italy

Received May 17, 1996[®]

A layered mercury telluride, Rb₂Hg₃Te₄, was discovered during an exploration of hydro(solvo)thermal synthesis of tellurides at temperatures somewhat above the boiling point of ethylenediamine. Crystals of Rb₂Hg₃Te₄ were grown from solvothermal reactions using ethylenediamine as a solvent. Single crystal X-ray diffraction analysis shows that this compound belongs to the orthorhombic system, space group *Pbcn* (No. 60) with lattice parameters $a = 12.177(2)$ Å, $b = 7.245(2)$ Å, $c = 14.545(2)$ Å, and $Z = 4$. The structure contains two-dimensional layers of $^{2-}_\infty[\text{Hg}_3\text{Te}_4^{2-}]$ which are separated by the Rb⁺ counterions. The interlayer Te–Te distances imply weak van der Waals interactions. Rb₂Hg₃Te₄ is the first two-dimensional mercury telluride prepared by an unconventional low-temperature technique.

Introduction

High-temperature routes represent the traditional ways for the syntheses of solid state materials. Important methods, such as condensation growth,¹ chemical vapor transport (CVT) growth,² vapor–liquid–solid (VLS) growth,³ flux growth,⁴ and solution alloy growth,⁵ have been used to grow crystals of many inorganic solids at relatively high temperatures. This situation is now rapidly changing. An increasing interest in low-temperature methods has led to extensive exploration of synthetic routes suitable for use at lower temperatures. In the area of chalcogenide chemistry, the development of the flux growth technique employing alkali metal polychalcogenide salts has resulted in a large number of new compounds over the past decade. Many of these are obtained at temperatures between 300 and 500 °C.⁶ Another promising technique that may work

at even lower temperatures makes use of hydro(solvo)thermal reactions.⁷ Such a reaction utilizes a solvent (such as water) under pressure and at temperatures usually below its critical temperature. Under hydro(solvo)thermal conditions, the solubility of the reactants increases significantly, enabling the reaction to take place at a much lower temperature. The technique has been widely used for preparation of many inorganic materials, such as zeolites, quartz, transition metal phosphates, oxides, and main group sulfides.⁸ Recently, it has also been applied to the synthesis of a variety of transition metal sulfides and selenides at rather low temperatures.⁹

[†] Henry Dreyfus Teacher-Scholar 1994–1998.

[®] Abstract published in *Advance ACS Abstracts*, January 15, 1997.

- (1) Pizzarello, F. *J. Appl. Phys.* **1954**, 25, 804. Hamilton, D. R. *J. Electrochem. Soc.* **1958**, 105, 735. Reizman, F.; Basseches, H. In *Metalurgy of Semiconducting Materials*; Schroeder, J. B., Ed.; Interscience: New York, 1962. Brenner, S. S. In *The Art and Science of Growing Crystals*; Gilman, J. J., Ed.; Wiley: New York, 1963. Krucheanu, E.; Nikulesku, D.; Vanku, A. *Sov. Phys.-Crystallogr. (Engl. Transl.)* **1965**, 9, 445. Gottlieb, G. E., Jr. *J. Electrochem. Soc.* **1965**, 112, 903.
- (2) Schäfer, H. *Chemical Transport Reactions*; Academic Press: New York, 1964. Nassau, K. In *Technique of Inorganic Chemistry*; Jonassen, H. B., Weissberger, A., Eds.; Interscience: 1968; Vol. III. Rosenberger, F. In *Preparation and Characterization of Materials*; Ronig, J. M., Rao, C. N. R., Eds.; Oxford University Press: Oxford, U.K., 1987.
- (3) Wagner, R. S.; Ellis, W. C.; Jackson, K. A.; Arnold, S. M. *J. Appl. Phys.* **1964**, 35, 2993. Wagner, R. S.; Ellis, W. C. *Trans. AIME* **1965**, 223, 1053.
- (4) Bloom, H. *The Chemistry of Molten Salts*; Benjamin: New York, 1967. *Molten Salts Handbook*; Janz, G. J., Ed.; Academic Press: New York, 1967. Mamantov, G. *Molten Salts: Characterization and Analysis*; Marcel Dekker: New York, 1969. Elwell, D.; Scheel, H. J. *Crystal Growth from High-Temperature Solutions*; Academic Press: London, 1975.
- (5) Kröger, F. A.; de Nobel, D. *J. Electron. Control* **1955**, 1, 190. Hall, R. N. *J. Appl. Phys.* **1958**, 29, 914. Wolff, G.; Keck, P. H.; Broder, J. D. *Phys. Rev.* **1959**, 94, 753. Lorenz, M. R. *J. Appl. Phys.* **1962**, 33, 3304.
- (6) See, for example, the most recent publications: McCarthy, T. J.; Kanatzidis, M. G. *Inorg. Chem.* **1995**, 34, 1257. Li, J.; Guo, H.-Y.; Zhang, X.; Kanatzidis, M. G. *Alloys Compounds* **1995**, 218, 1. McCarthy, T. J.; Tanzer, T. A.; Kanatzidis, M. G. *J. Am. Chem. Soc.* **1995**, 117, 1294. Zhang, X.; Park, Y.; Hogan, T.; Schindler, J. L.; Kannewurf, C. R.; Seong, S.; Albright, T.; Kanatzidis, M. G. *J. Am. Chem. Soc.* **1995**, 117, 10300, and the references cited therein. Li, J.; Guo, H.-Y.; Yglesias, R. A. *Chem. Mater.* **1995**, 7, 599, and the references cited therein. Li, J.; Guo, H.-Y.; Proserpio, D. M.; Sironi, A. *J. Solid State Chem.* **1995**, 117, 247. Zhang, X.; Li, J.; Foran, B.; Lee, S.; Guo, H.-Y.; Hogan, T.; Kannewurf, C. R.; Kanatzidis, M. G. *J. Am. Chem. Soc.* **1995**, 117, 10513. Li, J.; Liszewski, Y. Y.; Chen, F.; Mulley, S.; Proserpio, D. M. *Chem. Mater.* **1996**, 8, 598. Zhang, X.; Kanatzidis, M. G. *J. Am. Chem. Soc.* **1996**, 118, 693. Sutorik, A. C.; Albritton-Thomas, J.; Hogan, T.; Kannewurf, C. R.; Kanatzidis, M. G. *Chem. Mater.* **1996**, 8, 751. Chondroudis, K.; McCarthy, T. J.; Kanatzidis, M. G. *Inorg. Chem.* **1996**, 35, 840.
- (7) Laudise, R. A. *Progress in Inorganic Chemistry*; Interscience: New York, 1962; Vol. III. Barrer, R. M. *Hydrothermal Chemistry of Zeolites*; Academic Press: London, 1982. Rabenau, A. *Angew. Chem., Int. Ed. Engl.* **1985**, 24, 1026. Laudise, R. A. *Chem. Eng. News*, **1987**, 30 (Sep 28), 30–43.
- (8) See, for example: Praise, J. B. *J. Chem. Soc., Chem. Commun.* **1985**, 606. Sheldrick, W. S.; Kaub, J. Z. *Anorg. Allg. Chem.* **1986**, 535, 179. Lii, K. H.; Haushalter, R. C. *J. Solid State Chem.* **1987**, 69, 320. Haushalter, R. C.; Lai, F. W. *J. Solid State Chem.* **1988**, 76, 218. Sheldrick, W. S.; Hauser, H.-J. Z. *Anorg. Allg. Chem.* **1988**, 557, 105. Sheldrick, W. S. Z. *Anorg. Allg. Chem.* **1988**, 562, 23. Haushalter, R. C.; Lai, F. W. *Science* **1989**, 246, 1289. Mundi, L. A.; Strohmaier, K. G.; Goshorn, D. P.; Haushalter, R. C. *J. Am. Chem. Soc.* **1990**, 112, 8182. Haushalter, R. C.; Mundi, L. A. *Inorg. Chem.* **1990**, 29, 157. Parise, J. B. *J. Chem. Soc., Chem. Commun.* **1990**, 1553. Parise, J. B. *Science* **1991**, 251, 293. Haushalter, R. C.; Mundi, L. A. *Chem. Mater.* **1992**, 4, 31. Meyer, L. M.; Haushalter, R. C. *Chem. Mater.* **1994**, 6, 349.

Comparatively, few tellurides have been synthesized using low-temperature routes. Limited examples include binary RbTe₆,¹⁰ Cs₃Te₂₂,¹¹ Cs₂Te₁₃,¹² Cs₄Te₂₈,¹² ternary Cs₂SnTe₄,¹³ and quaternary K₂HgSnTe₄.¹⁴ During our investigation of the low-temperature synthesis of solid state materials, we have made a large effort to explore and understand the crystal growth of metal tellurides under hydro(solvo)thermal conditions. Using water and several organic solvents, we have successfully synthesized a group of novel mercury^{15a} and indium¹⁶ telluro-metalates. All of these are obtained at temperatures below 200 °C. The structures of these compounds are characterized by a common and unique feature: each incorporates a transition metal coordination complex as cation and a Zintl ion as anion. While low-temperature methods have produced mostly molecular and 1-D chain compounds,^{15b} we believe that hydro(solvo)thermal reactions are also promising for crystal growth of tellurides containing extended network structures. In this paper, we report the synthesis and structure determination of such an example, Rb₂Hg₃Te₄ (**I**).

Experimental Section

Materials. Iron(II) chloride (powder, 99.5%, AESAR/Johnson Matthey), mercury(I) chloride (powder, 99.5%, Fisher Scientific), Rb₂Te (prepared by reaction of Rb and Te in liquid ammonia¹⁷), HgTe (prepared by direct synthesis from Hg and Te at 200 °C), and Te (powder, 99.8%, Aldrich Chemical Co.) were used as starting materials. Ethylenediamine (99%, anhydrous; Fisher) was used as solvent.

Crystal Growth of Rb₂Hg₃Te₄. Single crystals of Rb₂Hg₃Te₄ (**I**) were first obtained from a solvothermal reaction containing 0.225 g (0.75 mmol) of Rb₂Te, 0.032 g (0.25 mmol) of FeCl₂, 0.059 g (0.125 mmol) of Hg₂Cl₂, and 0.096 g (0.75 mmol) of Te. The chemicals were weighed and mixed under inert atmosphere. The mixture was then transferred to a thick-wall Pyrex tube and approximately 0.2 mL of solvent (en) was added to the sample. After the liquid was condensed by liquid nitrogen, the tube was sealed with a torch under vacuum. The sample was heated at 180 °C for 7 days. After cooling to room temperature, the mixture was washed with 35 and 95% ethanol followed by drying with anhydrous diethyl ether. Quantitative amounts of black, column-like crystals of **I** were isolated from the final product. Analysis with the microprobe of a Kevex EDAX (energy dispersive analysis by X-ray) on a Hitachi S-2400 scanning electron microscope confirmed the presence of Rb, Hg, and Te in the approximate ratio 2:3.2:4.2. No other elements were detected. The exact composition of the compound was established from the X-ray structure determination.

Powder Sample Preparation. To obtain a single phase of **I**, polycrystalline samples were prepared by direct synthesis at various temperatures. In the first group of reactions (group A), a stoichiometric mixture of Rb₂Te, HgTe was weighed in a glovebox and evacuated and sealed in a ca. 5-in. long thin-walled Pyrex (or silica) tube. The reaction tubes were heated to 200, 400, 600, and 800 °C, respectively, and kept at these temperatures for 3 days. The final products were

Table 1. Crystallographic Data for Rb₂Hg₃Te₄

chem formula	Hg ₃ Rb ₂ Te ₄	V, Å ³	1283.2(4)
fw	1283.11	Z	4
space group	<i>Pbcn</i> (No. 60)	T, °C	20
a, Å	12.177(2)	λ, Å	0.710 73
b, Å	7.245(2)	ρ _{calc} , g cm ⁻³	6.642
c, Å	14.545(2)	μ, mm ⁻¹	52.195
R indices ^a [F _o > 4σ(F _o)] (989 data)	R1, 0.0340; R2 _w , 0.0583		
R indices ^b (all data)	R1, 0.0677; R2 _w , 0.0653		

^a R1 = Σ|F_o| - |F_c|/Σ|F_o|. ^b R2_w = [Σ(F_o² - F_c²)/ΣwF_o⁴]^{1/2}. Weighting: w = 1/[σ²(F_o²) + (0.0182P)² + 10.6709P], where P = (F_o² + 2F_c²)/3.

Table 2. Atomic Coordinates and Equivalent Isotropic Displacement Parameters (Å²) for Rb₂Hg₃Te₄

atom	x	y	z	U(eq) ^a
Hg(1)	0.343 84(5)	0.162 04(8)	0.244 95(4)	0.0380(2)
Hg(2)	0	0.100 02(11)	1/4	0.0351(2)
Te(1)	0.154 07(7)	0.331 16(13)	0.158 10(6)	0.0258(2)
Te(2)	0.424 05(8)	0.354 04(12)	0.388 54(6)	0.0274(2)
Rb	0.364 49(12)	0.838 3(2)	0.457 56(11)	0.0370(4)

^a U(eq) is defined as one-third of the trace of the orthogonalized U_{ij} tensor.

first washed by dimethylformamide (DMF) followed by absolute alcohol (100%) and dried by anhydrous diethyl ether. Dark, fine powders were formed in each case. No apparent attack of the reaction tube was observed. The starting materials for the second group of reactions (group B) were slightly different, where elemental Hg and Te were used instead of HgTe. The heating scheme was identical to the first set of reactions.

Single-Crystal X-ray Diffraction. A black needle crystal (0.16 × 0.05 × 0.05 mm) of **I** was mounted on a glass fiber in air on an Enraf-Nonius CAD4 automated diffractometer, and 25 intense reflections [17° < 2θ < 23°] were centered using graphite-monochromated Mo Kα radiation. Least-squares refinement of their setting angles resulted in the unit-cell parameters reported in Table 1, together with other details associated with data collection and refinement. Data were collected using the ω-scan method with a scan interval of 1.0°, within the limits 6° < 2θ < 54° for 0 ≤ h ≤ 15, 0 ≤ k ≤ 9, 0 ≤ l ≤ 18. The diffracted intensities were corrected for Lorentz and polarization effects and decay. An empirical absorption correction based on ψ-scans was applied to all data (transmission range 1.0 to 0.327). The structure was solved by direct methods with SIR92¹⁸ and refined by full-matrix least-squares on F_o² using all of the 1388 independent reflections and 43 parameters (for 1388 data collected). Anisotropic thermal displacements were assigned to all atoms, and an empirical extinction coefficient, as implemented in SHELX-93,¹⁹ was refined to a value of 0.000 52(3), giving a significant improvement in the agreement factors. The final difference electron density map shows no features with a height greater than 5% of a Rb atom. All calculations were performed using SHELX-93.¹⁹ Crystal drawings were produced with SCHAKAL.²⁰ Final atomic coordinates, average temperature factors, and selected bond lengths and angles are reported in Tables 2 and 3.

Results and Discussion

Synthesis. An oxidation–reduction process was involved in the synthesis of **I**. The oxidation state of each element in **I** is assigned as follows: Rb(I), Hg(II), and Te(–II). During the reaction, Hg₂²⁺ was oxidized to Hg²⁺, while elemental Te was reduced. Although Fe did not incorporate into the structure, FeCl₂ was found to be essential in the crystal growing process of **I**. The exact role of this species is not yet understood,

- (9) Liao, J.-H.; Kanatzidis, M. G. *J. Am. Chem. Soc.* **1990**, *112*, 7400.
- (10) Liao, J.-H.; Kanatzidis, M. G. *Inorg. Chem.* **1992**, *31*, 431.
- (11) Kim, K.-W.; Kanatzidis, M. G. *J. Am. Chem. Soc.* **1992**, *114*, 4878.
- (12) Wood, P. T.; Pennington, W. T.; Kolis, J. W. *J. Am. Chem. Soc.* **1992**, *114*, 9233.
- (13) Jerome, J. E.; Wood, P. T.; Pennington, W. T.; Kolis, J. W. *Inorg. Chem.* **1994**, *33*, 1556.
- (14) Jerome, J. E.; Wood, P. T.; Pennington, W. T.; Kolis, J. W. *Inorg. Chem.* **1994**, *33*, 1733.
- (15) Sheldrick, W. S.; Schaaf, B. Z. *Naturforsch.* **1994**, *49b*, 993.
- (16) Sheldrick, W. S.; Wachhold, M. *Angew. Chem., Int. Ed. Engl.* **1995**, *34*, 450.
- (17) Sheldrick, W. S.; Wachhold, M. *J. Chem. Soc., Chem. Commun.* **1996**, 607.
- (18) Sheldrick, W. S.; Schaaf, B. Z. *Naturforsch.* **1994**, *49b*, 57.
- (19) Dhinra, S. S.; Haushalter, R. C. *Chem. Mater.* **1994**, *6*, 2376.
- (20) (a) Li, J.; Rafferty, B. G.; Mulley, S.; Proserpio, D. M. *Inorg. Chem.* **1995**, *34*, 6417.
- (21) Chen, Z.; Li, J.; Mulley, S.; Proserpio, D. M. Manuscript in preparation.
- (22) (b) References cited in a.
- (23) Chen, Z.; Li, J.; Emge, T.; Proserpio, D. M. Manuscript in preparation.
- (24) Li, J.; Liszewski, Y. Y.; MacAdams, L. A.; Chen, F.; Mulley, S.; Proserpio, D. M. *Chem. Mater.* **1996**, *8*, 598.

- (18) Altomare, A.; Cascarano, G.; Giacovazzo, C.; Guagliardi, A.; Burla, M. C.; Polidori, G.; Camalli, M. *J. Appl. Crystallogr.* **1994**, *27*, 435.
- (19) Sheldrick, G. M. *SHELX-93*: program for structure refinement; University of Goettingen: Goettingen, Germany, 1994.
- (20) Keller, E. *SCHAKAL 92*: a computer program for the graphical representation of crystallographic models; University of Freiburg: Freiburg, Germany, 1992.

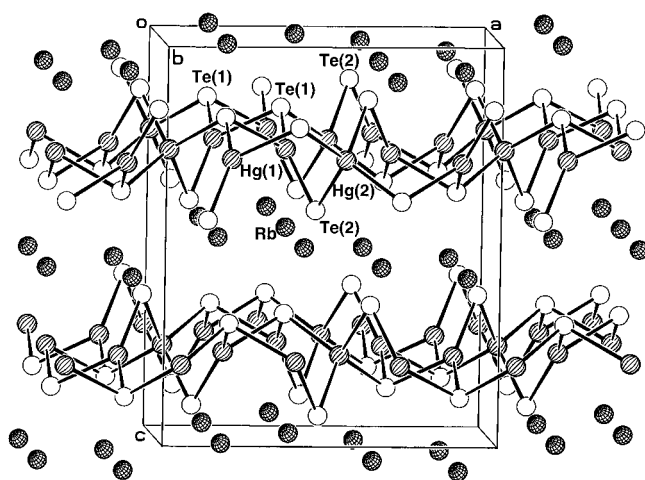


Figure 1. View of the unit cell content of $\text{Rb}_2\text{Hg}_3\text{Te}_4$ (**I**). The cross-hatched circles are Rb atoms, the shaded circles Hg, and the open circles Te.

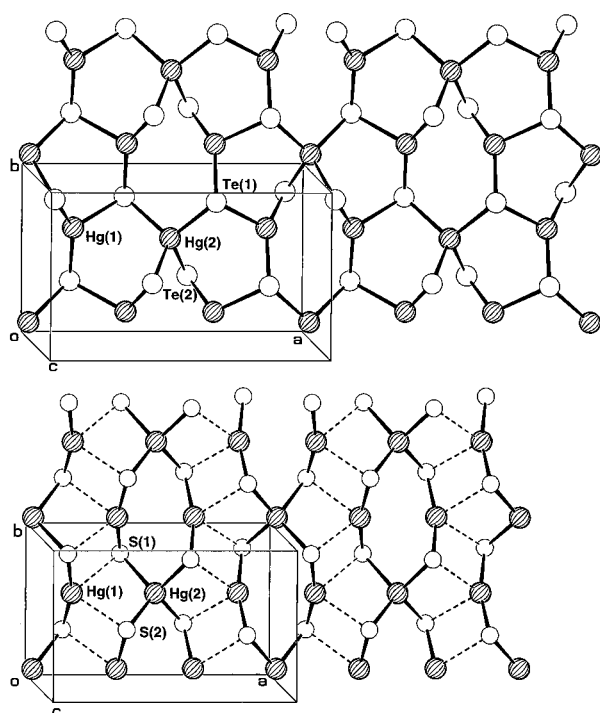


Figure 2. View of one layer of $[\text{Hg}_3\text{Te}_4]^{2-}$ in **I** (top) and the packing of chains of $[\text{Hg}_3\text{Q}_4]^{2-}$ in **II–IV** for $\text{Q} = \text{S}$ (bottom).

although possibly it acted as a reducing agent during the formation of **I**. The reactions were also very sensitive to other experimental conditions, such as temperature and the initial composition of the starting materials.^{15a}

Structure. $\text{Rb}_2\text{Hg}_3\text{Te}_4$ possesses a unique layered structure. As shown in Figure 1, it consists of the $[\text{Hg}_3\text{Te}_4]^{2-}$ two-dimensional network and Rb^+ cations that separate these layers. The shortest interlayer Te–Te distances are slightly longer than the sum of the van der Waals radii of 4.12 Å,²¹ which eliminates any significant Te–Te bonding interactions. The $[\text{Hg}_3\text{Te}_4]^{2-}$ layer is formed by interconnecting six- and eight-membered rings of alternating mercury and tellurium atoms, Hg_3Te_3 , and Hg_4Te_4 , (see Figure 2, top). The five-membered ring, Hg_2Te_3 , is commonly found in a number of molecular and 1-D mercury telluride compounds (see ref 15), but adjacent six- and eight-membered mercury–tellurium rings

Table 3. Selected Bond Lengths (Å) and Angles (deg) for $\text{Rb}_2\text{Hg}_3\text{Te}_4$ ^a

Hg(1)–Te(2)	2.6928(11)	Hg(1)–Te(1) ^a	2.7098(12)
Hg(1)–Te(1)	2.9047(11)		
Hg(2)–Te(2) ^a	2.8446(11)	Hg(2)–Te(2) ^b	2.8447(11)
Hg(2)–Te(1)	2.8480(11)	Hg(2)–Te(1) ^c	2.8480(11)
Te(2)–Hg(1)–Te(1) ^a	144.60(4)	Te(2)–Hg(1)–Te(1)	114.08(3)
Te(1) ^a –Hg(1)–Te(1)	100.25(3)		
Te(2) ^a –Hg(2)–Te(2) ^b	102.42(5)	Te(2) ^a –Hg(2)–Te(1)	119.12(3)
Te(2) ^b –Hg(2)–Te(1)	104.48(3)	Te(2) ^a –Hg(2)–Te(1) ^c	104.48(3)
Te(2) ^b –Hg(2)–Te(1) ^c	119.13(3)	Te(1)–Hg(2)–Te(1) ^c	107.97(5)

^a Symmetry transformations used to generate equivalent atoms (indicated by superscript a–c): (a) $-x + 1/2, y - 1/2, z$; (b) $x - 1/2, y - 1/2, -z + 1/2$; (c) $-x, y, -z + 1/2$.

are very rare. We believe such a structure motif has never been observed previously. There are two types of Hg in the structure. While Hg(2) forms a distorted tetrahedron with four long Hg–Te bonds, the coordination of Hg(1) to the three Te is planar and close to a T-shape, with two short and one long bond (see Table 3). The bond distances are comparable with tetracoordinated Hg found in $(\text{Hg}_4\text{Te}_{12})^{4-}$,²² $[\text{Hg}_3\text{Te}_7]^{4-}$,²³ and $(\text{HgTe}_8)^{2-}$ (2.69–2.97 Å).²⁴ Formal oxidation state assignment suggests that **I** is electron precise and is most likely a semiconductor.

Compound **I** is the first mercury telluride containing a two-dimensional network. The low-temperature methods so far have produced only molecular and chainlike mercury containing tellurides. Examples include $[\text{Hg}_2\text{Te}_5]^{2-}$,²² $(\text{Hg}_4\text{Te}_{12})^{4-}$,²² $[\text{Hg}_2\text{Te}_4]^{2-}$,²³ $[\text{Hg}_3\text{Te}_7]^{4-}$,²³ and $(\text{HgTe}_2)^{2-}$,²⁵ from solvent extraction of metal alloys; $(\text{HgTe}_8)^{2-}$,²⁴ $(\text{HgTe}_7)^{3-}$,²⁶ and $(\text{Hg}_4\text{Te}_{12})^{4-}$,²⁷ from nonaqueous solution phase reactions; and $(\text{Hg}_2\text{Te}_9)^{4-}$ and $[\text{Hg}_2\text{Te}_4]^{2-}$, from solvothermal reactions.¹⁵ Their crystal structures do not show any direct relation to **I**. Four known ternary alkali metal mercury chalcogenide compounds have the same stoichiometry ($\text{A}_2\text{Hg}_3\text{Q}_4$, where $\text{A} = \text{alkali metal}$, $\text{Q} = \text{S, Se}$). These are $\text{K}_2\text{Hg}_3\text{S}_4$ (**II**),²⁸ $\text{K}_2\text{Hg}_3\text{Se}_4$ (**III**),²⁸ $\text{Cs}_2\text{Hg}_3\text{Se}_4$ (**IV**),²⁹ and $\text{Na}_2\text{Hg}_3\text{S}_4$ (**V**).³⁰ In contrast to $\text{Rb}_2\text{Hg}_3\text{Te}_4$ however, all are unstable in moist air. Compounds **II–IV** are isostructural and contain chains of $[\text{Hg}_3\text{Q}_4]^{2-}$ (see **II** shown in Figure 2, bottom). Compound **V** consists of a highly corrugated layer structure $[\text{Hg}_3\text{S}_4]^{2-}$ based on 16-membered rings formed by alternating mercury and sulfur atoms. Compounds **II–IV** are related to **I** in the following way: they belong to the same space group as **I** (isotypic), and their 1-D chains pack along [100], forming layers similar to the 2-D layer of **I** (see Figure 2 for **I** and **II**). In the case of **I**, the bigger tellurium anions rearrange to connect the chains forming a unique layered structure. This results in a more expanded unit cell along a (averaged $a:b:c$ for **II** and **III**, 1.6:1:2.1; for **I**, 1.7:1:2.0). Compounds **I** and **II–IV** can also be viewed as derived from the ZnS structural type of HgS, HgSe, and HgTe (used as one of the possible precursors in our synthesis). The

- (22) Haushalter, R. C. *Angew. Chem., Int. Ed. Engl.* **1985**, *24*, 433.
- (23) Dhingra, S. S.; Warren, C. J.; Haushalter, R. C.; Bocarsly, A. B. *Chem. Mater.* **1994**, *6*, 2382.
- (24) Kanatzidis, M. G. *Comments Inorg. Chem.* **1990**, *10*, 161. Bollinger, J. C.; Roof, L. C.; Smith, D. M.; McConnachie, J. M.; Ibers, J. A. *Inorg. Chem.* **1995**, *34*, 1430.
- (25) Burns, R. C.; Corbett, J. D. *Inorg. Chem.* **1981**, *20*, 4433.
- (26) McConnachie, J. M.; Ansari, M. A.; Bollinger, J. C.; Ibers, J. A. *Inorg. Chem.* **1993**, *32*, 3201. Müller, U.; Grabe, C.; Neumüller, B.; Schreiner, B.; Dehnicke, K. *Z. Anorg. Allg. Chem.* **1993**, *619*, 500.
- (27) Kim, K.-W.; Kanatzidis, M. G. *Inorg. Chim. Acta* **1994**, *224*, 163.
- (28) Kanatzidis, M. G.; Park, Y. *Chem. Mater.* **1990**, *2*, 99.
- (29) Kanatzidis, M. G.; Sutorik, A. C. *Prog. Inorg. Chem.* **1995**, *43*, 151. No structural parameters are reported for $\text{Cs}_2\text{Hg}_3\text{Se}_4$ (**IV**).
- (30) Klepp, K. O. *J. Alloys Compounds* **1992**, *182*, 281.

(21) Bondi, A. J. *Phys. Chem.* **1964**, *68*, 441.

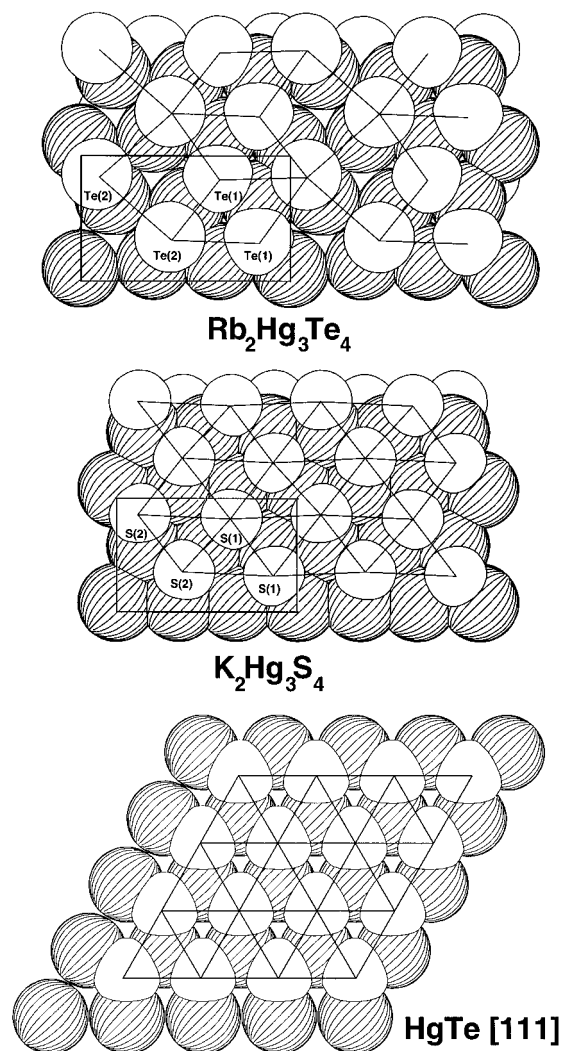


Figure 3. Packing diagrams for the layers shown in Figure 2, together with a section of the HgTe structure. The lines connect chalcogens atoms.

space-filling models of the layers of **I** and **II**, and a slice along [111] of HgTe (see Figure 3), show the similarities of the

hexagonal packing of Hg in all three compounds. Moreover, a comparison of Figures 2 and 3 shows that the bonding of Te distorts the hexagonal arrangement of the anions with respect to the more regular arrays of anions in **II** and HgTe. The striking difference between K₂Hg₃S₄ (**II**) and Na₂Hg₃S₄ (**V**) remains to be explained. The latter can be described as derived from a distorted-hexagonal close packed array of sulfur with Hg and Na filling the holes. This could probably be explained by the differences in ionic radii of the cations: Na(+1) = 1.16 Å, K(+1) = 1.52 Å, and Rb(+1) = 1.66 Å.³¹

Powder X-ray analysis was made on all samples prepared by direct synthesis at various temperatures (groups A and B). The ICDD inorganic database was used for identifying known phases present in the samples. The following results were obtained: At 200 °C, both groups A and B yielded primarily HgTe (~98%). At 400 °C, the reactions produced almost exclusively **I** (~98%).³² As the reaction temperature increased to 600 and 800 °C, **I** remained as the major phase (~70%) but another unknown phase was also found. The powder X-ray patterns of both samples (600 and 800 °C) contain the same peaks that could not be identified. Whether this unknown compound is a high-temperature phase or a decomposition product of **I** is not yet clear. Further investigations, including structure analysis and thermal studies, are planned.

Acknowledgment. This work was supported by the National Science Foundation via Grant DMR-9310431 and by the Camille and Henry Dreyfus Foundation through a Henry Dreyfus Teacher-Scholar Award. J.L. would like also to thank Rutgers University for partial support from a Research Council Grant.

Supporting Information Available: Summary of crystal data (Table S1), atomic coordinates (Table S2), complete list of interatomic distances and angles (Table S3), anisotropic thermal parameters (Table S4), and figures of a view of **I** showing thermal vibration ellipsoids and a plot of **V** (12 pages). Ordering information is given on any current masthead page.

IC960566H

(31) Shannon, R. D. *Acta Crystallogr.* **1976**, A32, 751.

(32) The powder X-ray patterns of all samples were compared with those generated from the single crystal data using LAZY and DBWS programs.